Interactive velocity analysis exercises

Jean-Claude Dulac

ABSTRACT

Stacking velocity analysis is performed by computing a coherency functional along hyperbolic trajectories. The properties of semblance, normalized mean, correlation, skewness and trimmed semblance are compared using an interactive program. Tests on a field common midpoint gather show that trimmed semblance gives better results than the other coherency functionals because it suppresses erratic data values. Furthermore the use of trimmed stack has improved the stack section of a real dataset with respect to mean stack.

INTRODUCTION

Shifted or missing traces occur often in common midpoint gathers. The simple mean stacking procedure incorrectly accounts for such traces, and does not filter abnormal amplitudes which sometimes result from crossing events.

Former studies include Woodward (1985) who examined differences between the mean and median stack and concluded that the median stacking procedure is a robust method which edits erratic values automatically. Muir and Claerbout (1973) studied the advantages of using the l_1 norm with erratic data. Haldorsen and Farmer (1989) propose the "trimmed stack" procedure to eliminate transient noise. Defining a trimmed stack challenges one to create a measure that will indicate what to discard. Computing a histogram of the amplitudes along the trajectory of the stack is the first step. Extracting a measure of the quality of a certain amplitude along this trajectory from the histogram comes second. Last, amplitudes which do not fit criteria for this measure are discarded.

In velocity analysis, the issue of "bad" traces and associated statistical problems is familiar. Sguazzero and Vesnaver (1986) surveyed methods frequently used to measure coherency of the amplitudes along the velocity analysis trajectories. I wanted to understand the behavior of coherency functionals in different events and to introduce new coherency measures, using an interactive program that helps to visualize the different functions on picked events. Following Clarebout (1989) who stresses that interactivity is one of the simplest, most powerful ways to test simple hypothesis, I wrote two programs using the graphic interface "gi" (Claerbout, 1989).

The first program simplifies testing standard and new measures on selected events. The second allows to filter dipping events and to visualize the effects of filtering upon the selected measures. Results of this statistical study are presented below. Part I gives a brief overview of the coherency functionals. Part II presents a stacking procedure which use statistical informations to edit bad data values automatically. Part III shows the effect of dip filtering on statistical measures.

COHERENCY FUNCTIONALS

Finding a measure and then determining which amplitudes are "good" or "bad" is a challenge. Addressing this problem I wrote an interactive program using "gi" to analyze the behavior of the different coherency measures used in stacking velocity analysis. For a picked hyperbola in the CMP section, the program (Figure 1) displays

1. a histogram of the amplitudes along the event,
2. the wiggle trace of the amplitudes along the event,
3. a plot of the coherency measures for a range of velocities around the velocity picked by the user,
4. and a plot of the kurtosis values of the histograms computed for the velocity analysis (Gray, 1979).

Statistical information

Analysis is performed in the offset-time domain (x,t) on one CMP gather, $d = d(x,t)$, where t is the two-way traveltime, x is the source receiver offset, and d is the observed wave field. Two steps make up the velocity analysis, repeated for every stacking velocity v:

1. Transformation of the non-zero-offset d data into zero-offset data d_0 by NMO-correction:
$$d_0 = d_0(x, t_0; v) = d(x, T(x; t_0, v)),$$
where $T(x)$ is given by the equation
$$T^2(x; t_0, v)) = t_0^2 + \frac{x^2}{v^2}.$$

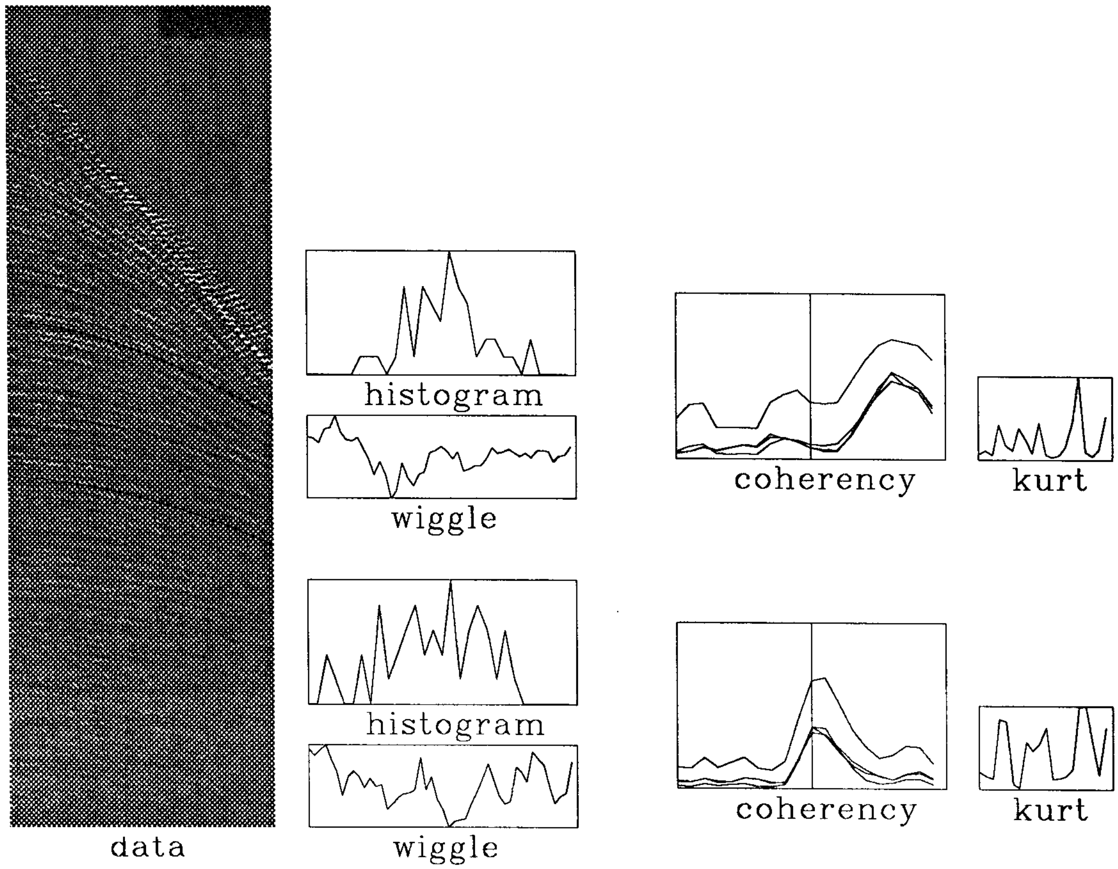

FIG. 1. "gi" hard copy of a velocity analysis session. Two different coherency measures are performed on two separate events. The lower panel is related to the upper event. The coherency curves are based on 20 velocity points spaced at 0.05 km/s around the user-picked velocity. Both the former and the velocity determined automatically by taking the maximum of coherency are close to one another. Coherency analysis in each panel gives the same results: shapes of the curves are almost identical, those of histograms are almost Gaussian. The "kurt" graph shows the kurtosis values of the different histograms computed on the velocity analysis trajectories.

2. For each traveltime t_0, the uniformity of the data $d_0(x, t_0; v)$ is evaluated by coherency functionals.

The most common functional measures are based on either summation of the traces or correlation of the traces with various choice of normalization (Sguazzero and Vesnaver, 1986). The simplest measure is the *mean amplitude* of the NMO-corrected traces from the near offset $x = x_0$ to the far offset $x = X$, averaged over time, i.e.,

$$\sum_{t=t_0-\delta/2}^{t_0+\delta/2} \left| \frac{1}{N_x} \sum_{x=x_0}^{X} d_0(x,t;v) \right| .$$

A normalized version of this equation provides the *normalized mean amplitude* estimator

$$\frac{\sum_{t=t_0-\delta/2}^{t_0+\delta/2} \left| \frac{1}{N_x} \sum_{x=x_0}^{X} d_0(x,t;v) \right|}{\sum_{t=t_0-\delta/2}^{t_0+\delta/2} \frac{1}{N_x} \sum_{x=x_0}^{X} |d_0(x,t;v)|} .$$

Another widely used coherency measure is *semblance*

$$\frac{\sum_{t=t_0-\delta/2}^{t_0+\delta/2} \left[\frac{1}{N_x} \sum_{x=x_0}^{X} d_0(x,t;v) \right]^2}{\sum_{t=t_0-\delta/2}^{t_0+\delta/2} \frac{1}{N_x} \sum_{x=x_0}^{X} [d_0(x,t;v)]^2} .$$

A different approach using spatial distribution information about the event, uses the *correlation* functional

$$\frac{2}{N_X(N_X-1)} \sum_{x=x_0}^{X} \sum_{y>x}^{X} \sum_{t=t_0-\delta/2}^{t_0+\delta/2} d_0(x,t;v) d_0(y,t;v),$$

or the *statistically-normalized correlation* functional

$$\frac{2}{N_X(N_X-1)} \sum_{x=x_0}^{X} \sum_{y>x}^{X} \frac{\sum_{t=t_0-\delta/2}^{t_0+\delta/2} d_0(x,t;v) d_0(y,t;v)}{\left[\sum_{t=t_0-\delta/2}^{t_0+\delta/2} d_0(x,t;v)^2\right]^{\frac{1}{2}} \left[\sum_{t=t_0-\delta/2}^{t_0+\delta/2} d_0(y,t;v)^2\right]^{\frac{1}{2}}} .$$

The latter is a measure of the continuity of signal shape across offset, while the semblance estimator depends equally upon signal shape and amplitude. The next step is to use complex coherency functionals on the analytic trace D and D_0, the *statistically normalized complex correlation* functional

$$\frac{2}{N_X(N_X-1)} \sum_{x=x_0}^{X} \sum_{y>x}^{X} \frac{\sum_{t=t_0-\delta/2}^{t_0+\delta/2} \overline{D_0}(x,t;v) D_0(y,t;v)}{\left[\sum_{t=t_0-\delta/2}^{t_0+\delta/2} D_0(x,t;v)^2\right]^{\frac{1}{2}} \left[\sum_{t=t_0-\delta/2}^{t_0+\delta/2} D_0(y,t;v)^2\right]^{\frac{1}{2}}} ,$$

where $\overline{D}$ denotes complex conjugation, to permit clear separation of amplitude and phase information.

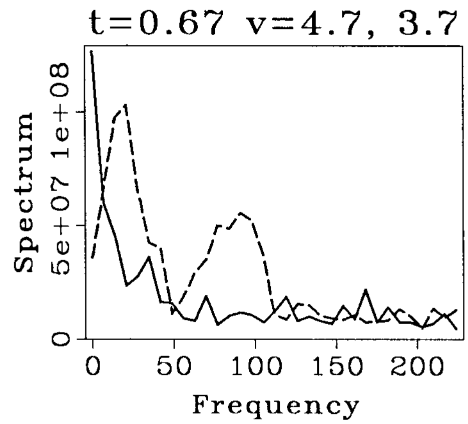

FIG. 2. Spectrum along offset for different velocities. Represented by the plain line, the spectrum has been computed along the NMO trajectory determined by the correct velocity (4.7 km/s). The broken line is the spectrum off the event.

Spectral information

Examination of the spatial spectrum along the stacking trajectory or along hyperbola allows me to measure amplitude variations along the trajectory. A sharp peak at zero frequency with fast decay (Figure 2) is a feature of the spectrum along an event. If the trajectory crosses an event with another dip (Figures 2, 12) I must see a second peak at larger frequency. I want a measure that discriminates between the sharpness of the first peak and the peaks away from the zero wavenumber. I choose to measure this property by using the skewness

$$\frac{\sum_k (S(k;v) - m)^3}{N_k * \sigma^3},$$

where m and σ^2 are the mean and variance of the spectrum. S represents the average spectrum on a window around the hyperbolic trajectory

$$S(k;v) = \frac{1}{\delta} \sum_{t=t_0-\delta/2}^{t_0+\delta/2} D_0(k,t;v),$$

where $D_0(k,t;v)$ is the spectrum along the hyperbolic trajectory and k represents spatial wavenumber. We compute the skewness for different velocities v to obtain yet another measure of the coherency.

Interpretation

Figures 1 and 3 do not allow me to see difference between the coherency analysis obtained from the semblance, correlation, or complex correlation measures. The normalized mean coherency functional always matches the same peaks as other coherency functionals. Figure 4 shows that correlation functionals give better results than semblance and the mean at deeper parts of the section. Through Figure 1,

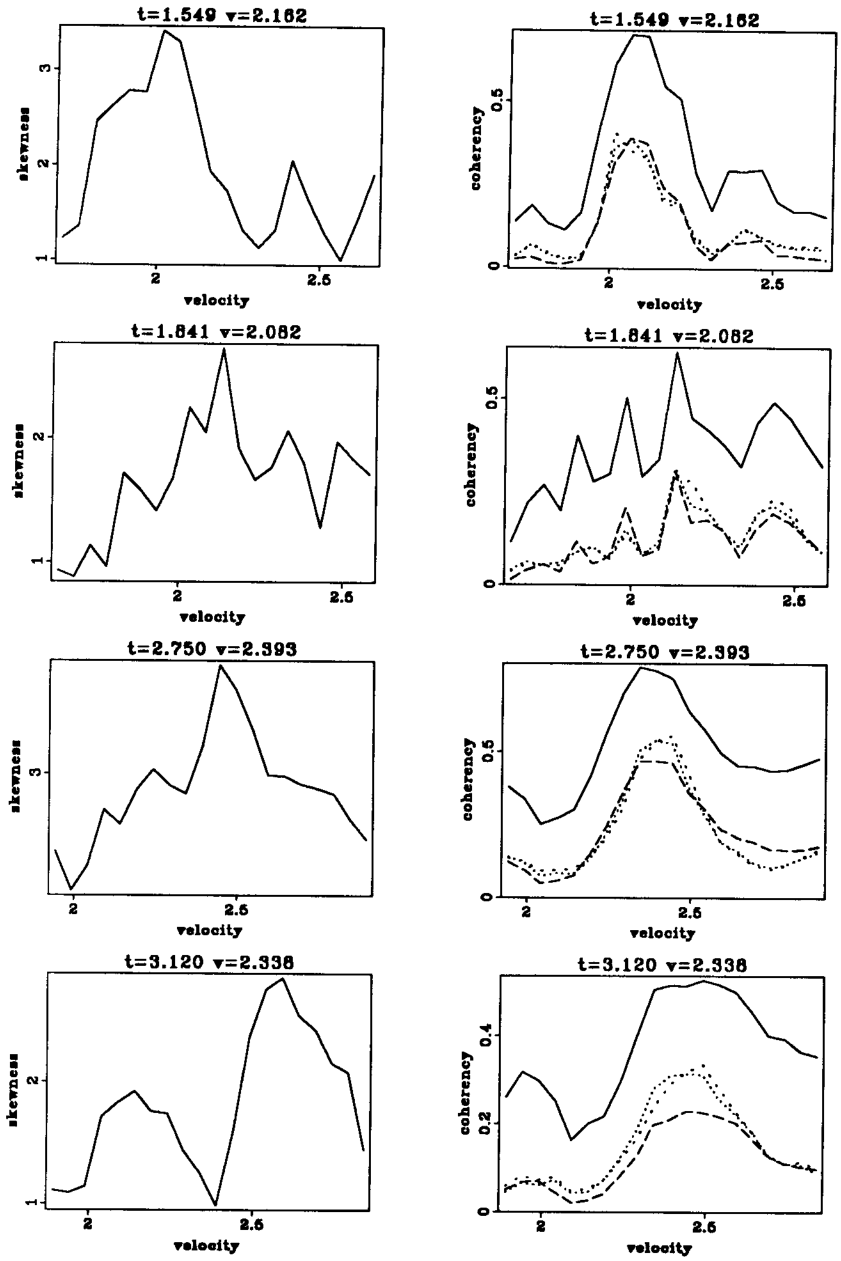

FIG. 3. Coherency functionals. Plots of the different coherency measures and the skewness for different events picked on the figure 1 shot gather. The right column shows normalized mean by a plain line, semblance in broken line, and the correlations in dotted lines (Large dots interval for normalized complex correlation). The left column represents skewness panels for the same event and the same range of velocities as the coherency graph. No differences can be noted between the coherency analysis obtained from the semblance or correlations measures. The peak of the skewness matches the maximum of the other coherency functionals.

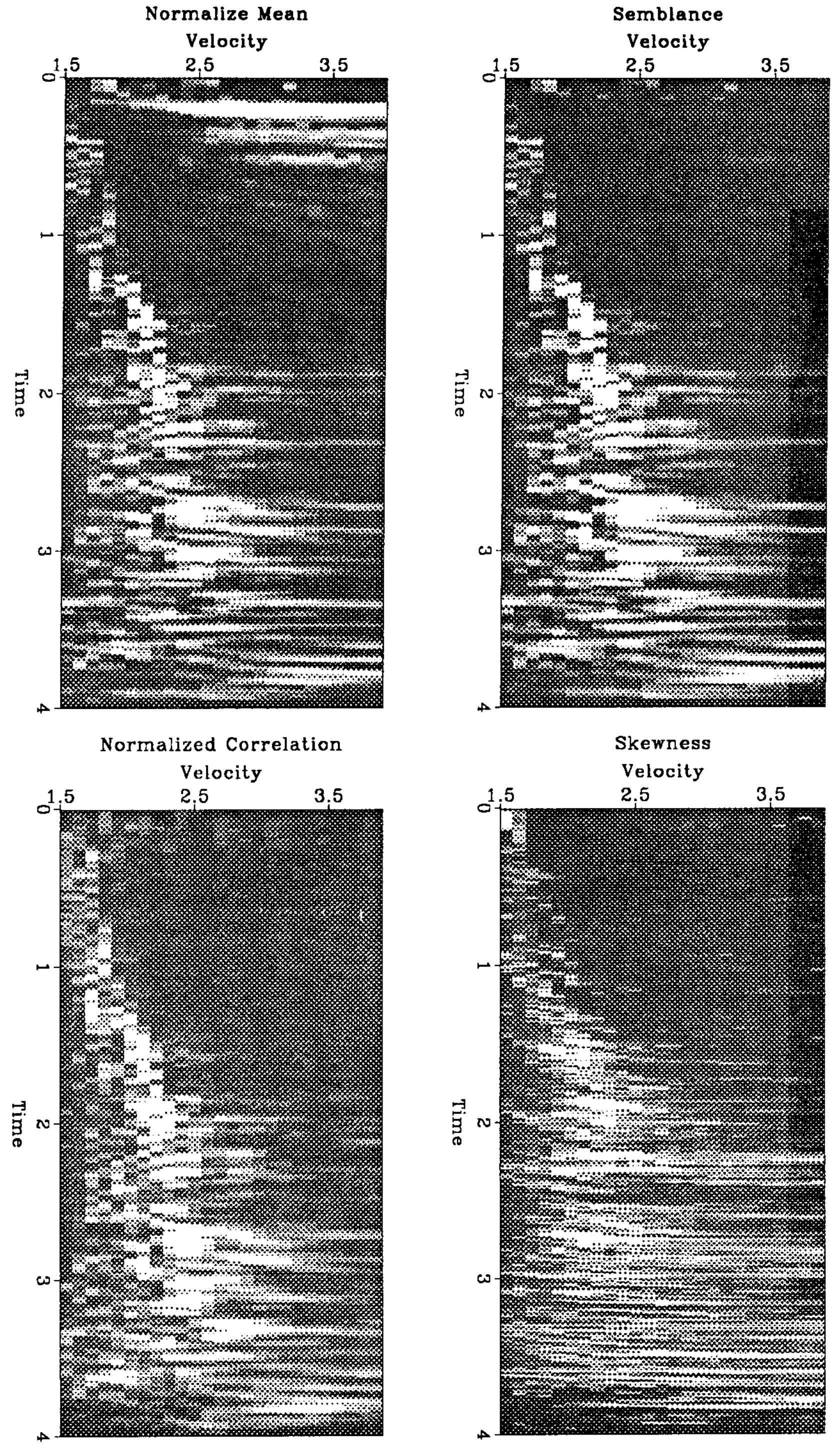

FIG. 4. Coherency functionals. Velocity analysis panels of the Figure 1 shot gather for different coherency functionals. The skewness velocity panel has a good time resolution; the correlation functional gives better picks than semblance.

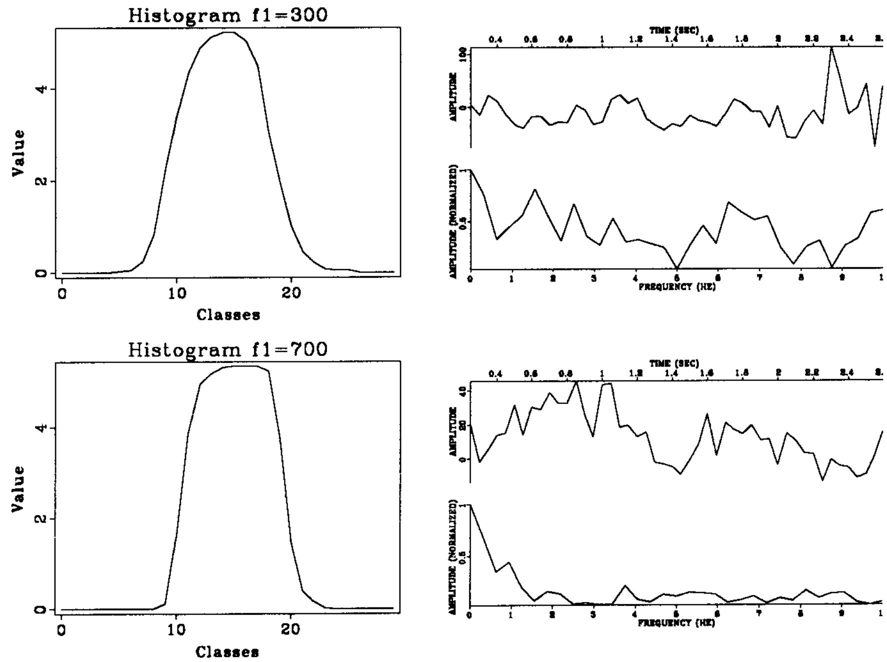

FIG. 5. Histogram of amplitudes and spectrum. At bell-shaped histogram corresponds a random spectrum. At flat histogram corresponds a uniform distribution

and the program itself, I can see that the coherency peak gives a velocity where the histogram along the NMO trajectory is like a Gaussian curve. The maximum of the skewness matches well the coherency functionals extreme. The skewness peak is often sharper than the other coherency functionals. At deeper parts of the section however, where the reflection signal gets weak, the spectrum becomes more random and the skewness does not show higher isolated peak than the semblance (Figure 4).

STACK

Criteria to choose "good" or "bad" amplitudes can be deduced from the generalized Gaussian shape of the histogram (Gray, 1979). Figure 5 represents a series of histograms associated with the spatial spectrum taken at different times. These histograms have been averaged in time and smoothed in offset. (A histogram is flat when the spectrum has a sharp peak at the origin and has a Gaussian distribution when the spectrum is more random.) From these observation, it can be assumed that all valid amplitudes lie in a certain range around the mean value. I apply this result to a stacking procedure. The stack is equivalent to a "trimmed mean stack" (Haldorsen and Farmer, 1989) but modified to be the trimmed weighted stack

$$\frac{1}{N-K}\sum_{i=K}^{N-K} d_0(x_i,t;v) \times p(x_i),$$

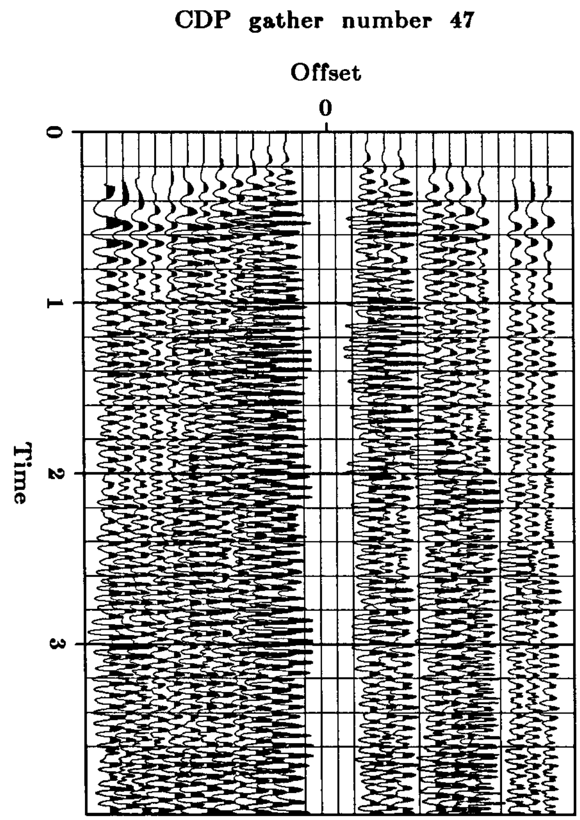

FIG. 6. Moveout corrected gather. On this gather, there are missing traces, high amplitude noise spikes and over-corrected events.

where N is the number of samples included in the summation, and K represents the quantile suppressed from the distribution. $p(x)$ is the probability distribution function of the amplitudes along offset.

Figure 6 illustrate the problem of "bad" amplitudes by showing a Vibroseis survey on land (Data courtesy of Chevron). Inner offsets have been contaminated with high amplitude noise spikes; there are some missing traces. Figure 7 shows mean and trimmed weighted stacks and yields these remarks:

1. Reflector continuity is increased relative to the mean stack. This procedure occurs between the mean and median processing compared by Woodward (1985). Where no cuts are done the stack is equivalent to a mean stack. Take a quantile equal to one-half the number of all classes of amplitude and the median stack results (Dellinger, 1984). Using the quantile approach to filter erratic data values, no assumptions are made on Gaussian probability distribution of the amplitudes. Looking also at the continuity and shape of the histogram used as weight (Figure 5), I may conclude that the "trimmed weighted stack" method is robust in rejecting "bad" amplitudes.

2. The high frequency content of the trimmed weighted stack is larger than that of the mean stack. Woodward (1985) points out "the mean is a linear operator

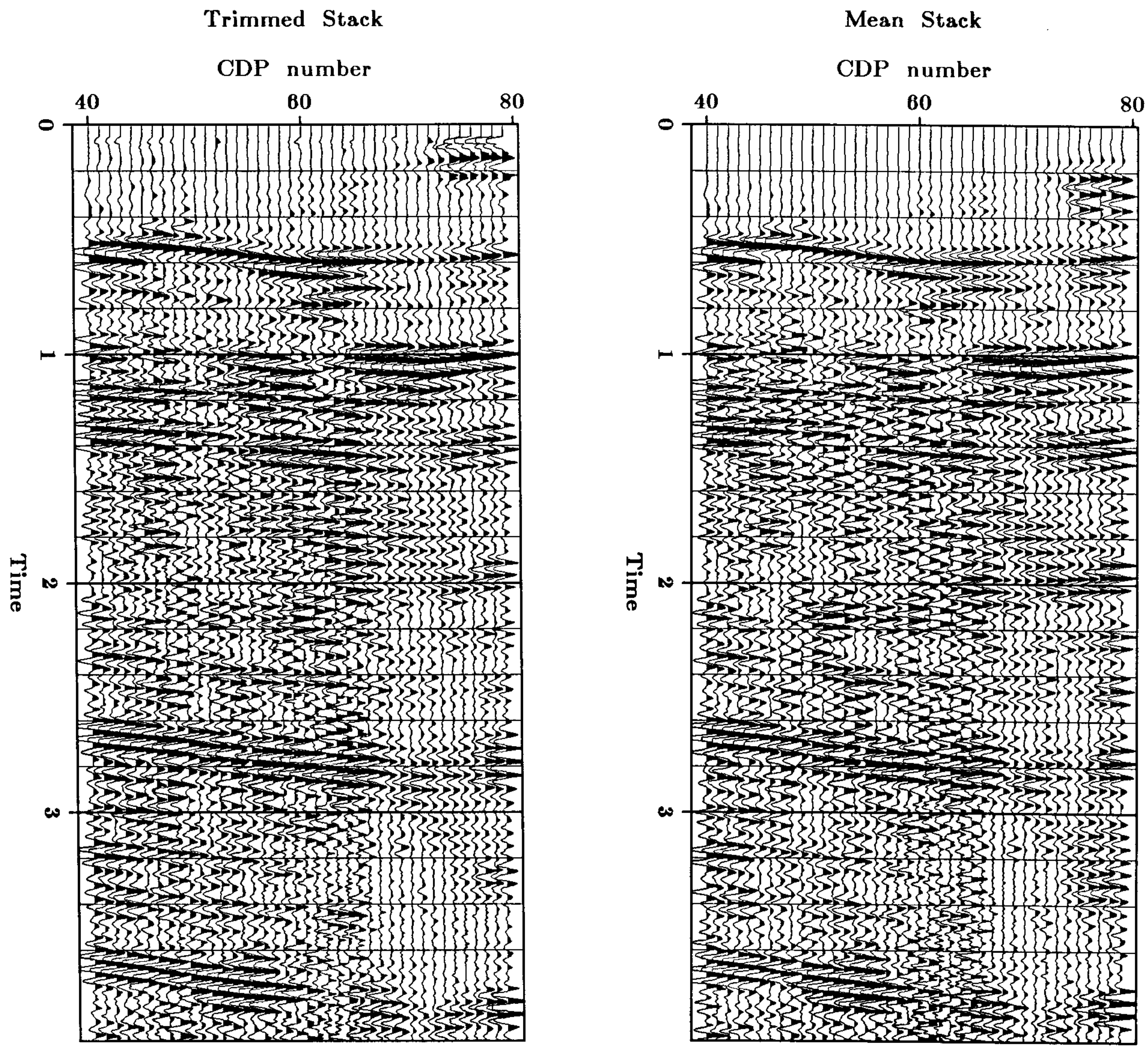

FIG. 7. Conventional stack and trimmed stack: inner offsets. The quantile chosen to do trimmed stack is equal to 5%. Sections were balanced after stack for display purposes. The trimmed stack section shows a better continuity of the events around 1 second and 3.5 seconds. The signal is more coherent in the region between the CDP numbers 54 and 68 and the time window 1, 2 seconds.

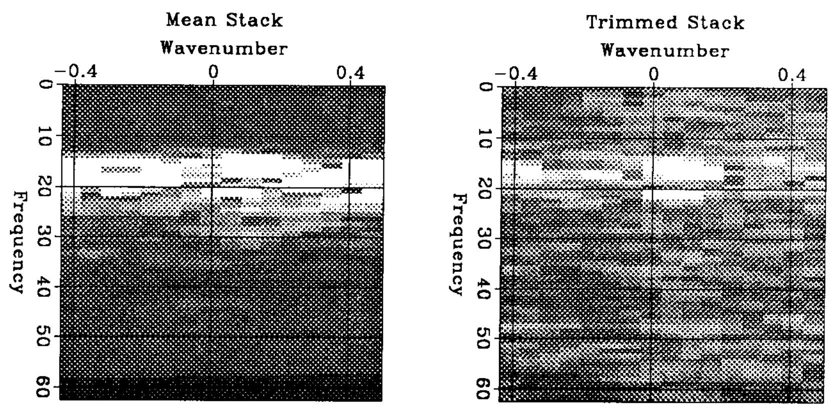

FIG. 8. 2-D spectra of the conventional and trimmed stacks. These images have been computed in the region between the CDP numbers 54 and 68, and the time window 1, 1.5 seconds and plotted with the same clip. On the trimmed stack spectrum, the energy is more concentrated around zero wavenumber, confirming the impression of greater lateral continuity of events in Figure 7.

and preserves the anti-alias filtered frequency spectrum of the data." The trimmed weighted stack samples across offset and is a non-linear operator. Figure 8 compares amplitude spectra of the two stacks. The spectrum of the weighted mean stack shows more continuous frequencies, and at wavenumber zero a more focused maximum than that of the mean stack.

An equivalent procedure can be applied during the velocity analysis. A trimmed semblance Figure 9) is computed only with the "good" amplitudes. A certain quantile is suppressed from the amplitude distribution and the "good" amplitudes are the non-rejected amplitudes. On the velocity panel processed with the trimmed semblance the focalization of the peak is increased relative to the semblance velocity panel.

These two examples show that the trim procedure improves the stack and the velocity analysis. For a low computational cost this procedure edits "bad" data values automatically.

FILTERING

Curious about the effects of filtering, I wrote a second interactive program using "gi", where the user can dip filter (Hale and Claerbout, 1983) the data or do a velocity analysis on the dip-filtered and non-dip-filtered data panels to examine differences. The program (Figure 10) displays:

1. the histogram of amplitudes along the event;

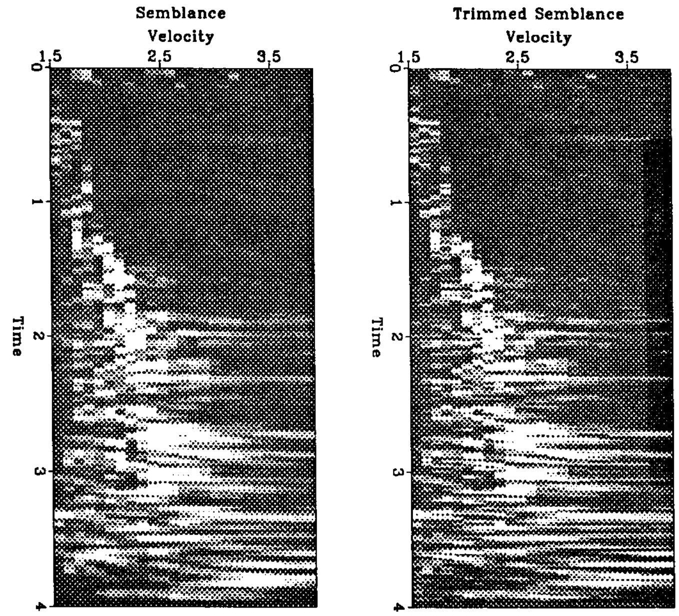

FIG. 9. Velocity analysis. The velocity analysis processes with the trimmed semblance procedure shows a better focalization of the peak. The quantile chosen to do trimmed semblance was equal to 5%. The section is the same than the one used for Figure 4.

2. a plot of the mean, semblance and skewness for a range of velocities centered at the velocity picked by the user;
3. the spectrum along the current trajectory;
4. and the dip-filtered data along a user-specified dip. The data can be iteratively filtered for many dips.

Depending upon user selection, either raw data or dip-filtered data can be used to make the different computations. Slope is specified by drawing a dip-line anywhere along the data. Range of frequencies and the attenuation of the dip filter are fixed by the program. (Giving the user the possibility of choosing a dip range would be an improvement of the program capacity.) Users can now match the coherency measures and event itself by dragging the mouse around the picked event.

As expected, the spectrum along the event shows a second peak which disappears when we do dip filtering (Figure 12). The difference between the evaluation of coherency functionals done on the two sections is minimal (Figures 10,11), while the trimmed semblance done on the dip-filtered data has a much sharper peak that the semblance computed on the non-dip-filtered data. This shows again the efficacy of the trimmed semblance.

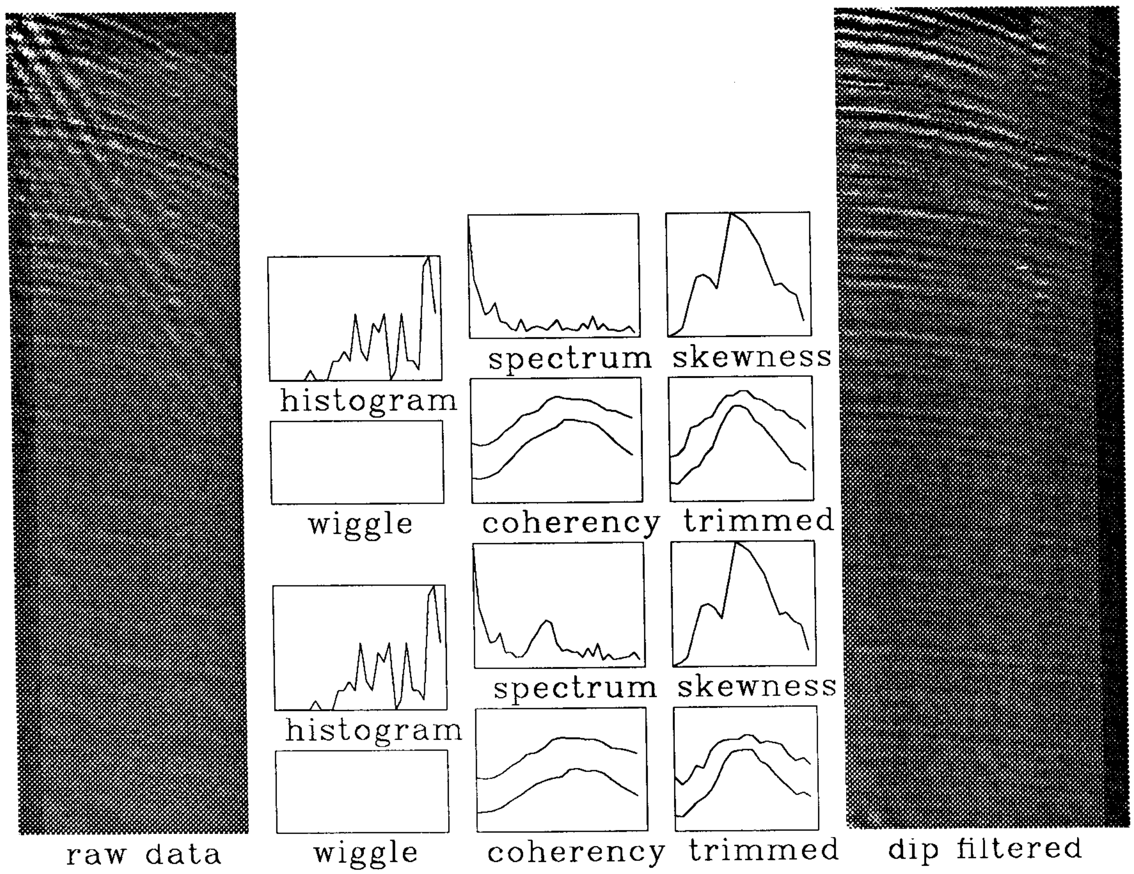

FIG. 10. "gi" hard copy of a user session. Raw data appears on the left; dip-filtered data is seen at the right. Dipping linear events are due to interference effects. Spectrum along the trajectory is shown. The skewness, mean and semblance have been computed on the events shown on the data. The bottom panel corresponds to the analysis of the event in the raw data; the top panel shows analysis of the event in the dip filtered data. A trimmed procedure comparable to the one used into the stacking procedure has been applied at computation of the "trimmed" coherency functional graph. In the "coherency" and "trimmed" graph semblance is the lower curve, normalized mean is the upper curve.

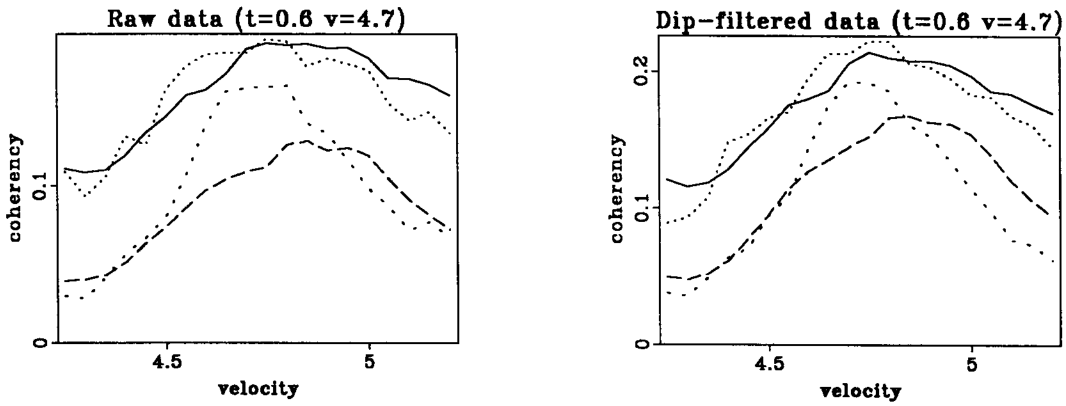

FIG. 11. Velocity analysis on raw and dip-filtered data. The graphs have been computed on the events shown Figure 10. The left graph has been computed with the raw data, the right one with dip-filtered data. The plain and broken lines represents the mean and the semblance. The dotted lines represent the trimmed mean and trimmed semblance (Large dots interval for trimmed semblance). The trimmed coherency functionals shows sharper peaks that the non-trimmed one.

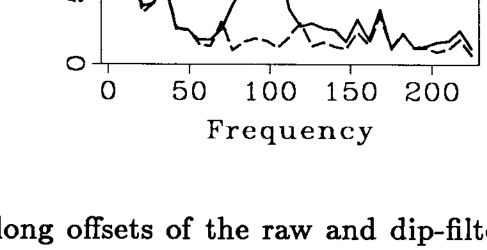

FIG. 12. Spectrum along offsets of the raw and dip-filtered data. The spectrums have been computed on the events shown Figure 10. The plain line represents the raw data spectrum. The second peak coming from the crossing event disappears on the dip-filtered data spectrum.

STATUS OF WORK

Writting these simple programs helps me to better understand geophysical problems. Both the speed and accuracy of the coherency functional program analysis leads me to believe that semblance is the best technique at reasonable cost. Trimmed semblance increased the accuracy of semblance by introducing some spatial information. The dip-filter program allows us to understand the action of a filter by visualization, and to see the frequency domain information. This program may be simply used to perform dip-filtering interactively. Interaction helps us to see the relation between event and operations. I avoid using synthetic data.

The trimmed weighted stack procedure is a robust method that edit bad amplitudes automatically. More work needs to be done to improve computation of the histogram with hypotheses like spatial and time stability. I also want to test for improvement of the stack procedure by using statistical information on the amplitudes and on trace phases.

ACKNOWLEDGMENTS

My thanks to Clement Kostov for his enthusiasm, interest and willingness to brainstorm. I am grateful to TOTAL CFP for supporting my study at Stanford. Additional thanks to J.J Raoult for encouraging me and suggesting ideas to me.

REFERENCES

Claerbout J.F., 1989, Interface for system independent plotting: SEP–**60**.

Claerbout J.F. and Muir F., 1973, Robust modeling with erratic data: Geophysics, **38**, 826-844.

Dellinger J., 1984, What is the median of {1,2,3,5}? : SEP–**41**, p. 409-413.

Gray W.B., 1979, Variable norm deconvolution: SEP–**19**.

Haldorsen J.B.U. and Farmer P.A., 1989, Suppression of high-energy noise using an alternative stacking procedure: Geophysics, **54**, 181-190.

Hale I.D. and Claerbout J.F., 1983, Butterworth dip-filters: Geophysics, **48**, 1033-1038.

Sguazzero P. and Vesnaver A., A comparative analysis of algorithms for stacking velocity estimation, *in* Bernabini M., Carrin P., Jacovitti G., Rocca F., Treitel S., Worthington M.H., Ed., 1986, Deconvolution and Inversion: Blackwell Scientific Publications, 267-286.

Woodward M.J., 1985, Statistical averages for velocity analysis and stack: Median vs. Mean: SEP–**42**, p. 97-111.

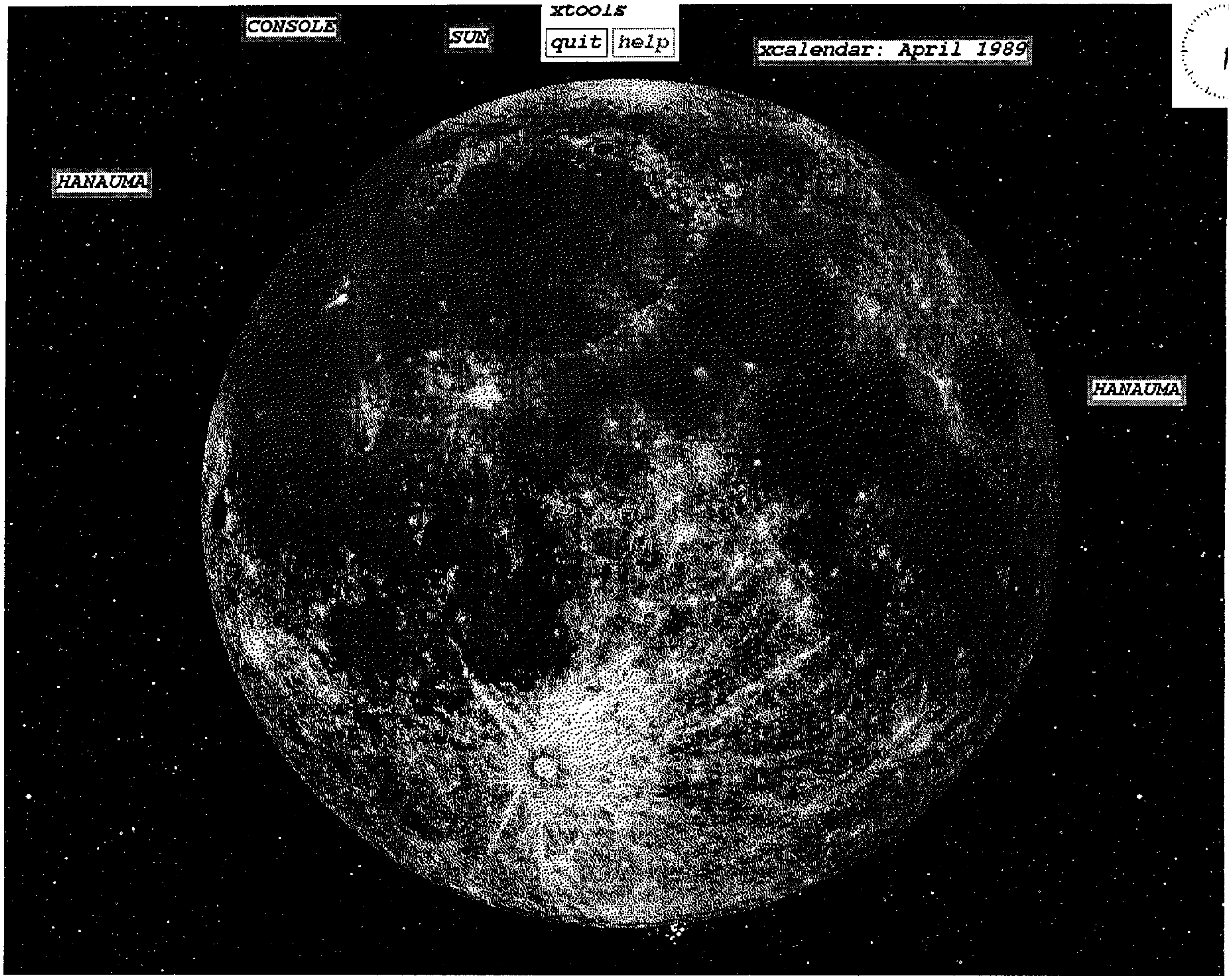
CONSOLE
SUN
xtools
quit
help
xcalendar: April 1989
HANAUMA
HANAUMA